NANO LETTERS

Letter

pubs.acs.org/NanoLett

The Unusual Mechanism of Partial Fermi Level Pinning at Metal–MoS_2 Interfaces

Cheng Gong,[†] Luigi Colombo,[‡] Robert M. Wallace,[†] and Kyeongjae Cho*,[†]

[†]Department of Materials Science and Engineering, The University of Texas at Dallas, Richardson, Texas 75080, United States

[‡]Texas Instruments, Dallas, Texas 75243, United States

Supporting Information

ABSTRACT: Density functional theory calculations are performed to unravel the nature of the contact between metal electrodes and monolayer MoS_2. Schottky barriers are shown to be present for a variety of metals with the work functions spanning over 4.2–6.1 eV. Except for the p-type Schottky contact with platinum, the Fermi levels in all of the studied metal–MoS_2 complexes are situated above the midgap of MoS_2. The mechanism of the Fermi level pinning at metal–MoS_2 contact is shown to be unique for metal–2D-semiconductor interfaces, remarkably different from the well-known Bardeen pinning effect, metal-induced gap states, and defect/disorder induced gap states, which are applicable to traditional metal–semiconductor junctions. At metal–MoS_2 interfaces, the Fermi level is partially pinned as a result of two interface behaviors: first by a metal work function modification by interface dipole formation due to the charge redistribution, and second by the production of gap states mainly of Mo d-orbitals character by the weakened intralayer S–Mo bonding due to the interface metal–S interaction. This finding would provide guidance to develop approaches to form Ohmic contact to MoS_2.

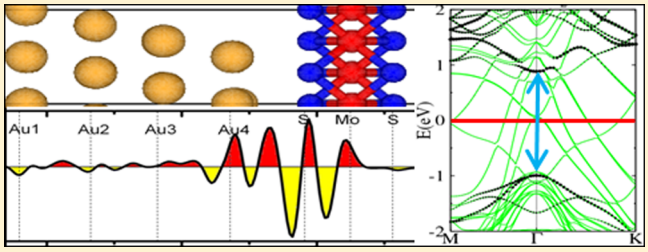

KEYWORDS: *MoS_2, metal contact, Fermi level pinning, Schottky barrier, work function, density functional theory (DFT)*

Monolayer transition metal dichalcogenides (TMDs) have drawn much interest in electronics since the demonstration of single-layer MoS_2 field effect transistors (FETs) with appealing performance a few years ago.[1] Single-layer MoS_2 with a sizable direct band gap exhibits a high on/off current ratio of about 10^8 and a high room-temperature carrier mobility upon scattering suppression through dielectric engineering.[2] The ultrathin thickness and inherent intralayer bonding property without surface dangling bonds make MoS_2 advantageous for scaled FETs because of smaller short channel effects,[3] absence of gap states when in contact with dielectrics, and excellent electrostatic control. Although MoS_2 exhibits fascinating intrinsic properties for electronics, contacts may severely limit the device performance.

The nature of the metal–MoS_2 contact (Ohmic or Schottky, n- or p-type) is still in much debate with contrasting experimental outcomes, and the underlying mechanisms for contact formation are not well understood yet. For example, although all MoS_2 FETs with Au electrodes are reported as n-type, controversy remains as to whether it is an Ohmic contact[1,4] or a Schottky contact.[5,6] While Pd is collectively claimed to form a Schottky contact with multilayer MoS_2, Fontana et al. concluded p-type[6] behavior and Neal et al. declared n-type.[4] Besides the fact that MoS_2 samples with different thicknesses and also unknown amounts of defects are utilized among laboratories, it is important to note that all these experiments are often room-temperature measurements in which thermionic emission may obscure the presence of small Schottky barrier heights (SBH). Qiu et al.[7] carried out a temperature-dependent study of bilayer MoS_2 FET with titanium contacts and found an n-type Ohmic contact at room temperature, while a Schottky contact with ~65 meV SBH for electron injection is noted for the same device by low-temperature measurements. On the basis of a temperature-dependent study with multilayer MoS_2, Saptarshi et al.[5] concluded universally that all metals, including low work function (WF) metal scandium (3.5 eV) and high WF metal platinum (5.9 eV), favor n-type Schottky contacts, with the Fermi levels (FLs) pinned close to the conduction band. Saptarshi et al. argued that the apparent linear dependence of current with drain voltage had misled researchers to believe that a truly Ohmic contact had already been achieved. In their work, the constant observation of Schottky contacts among a variety of metals with a WF difference larger than 2 eV suggests an interesting Fermi level pinning (FLP) behavior that is still elusive as for the origin. In fact, one recent theoretical study[8] predicted a partial FLP behavior based on a comparative study of monolayer MoS_2 interfacing with Ir, Pd, and Ru, but the detailed pinning mechanism was not elucidated. Another theoretical study was focused on the electronic states at Au– and Ti–MoS_2 interfaces, instead of on the Schottky barrier formation.[9]

Received: September 16, 2013
Revised: March 19, 2014
Published: March 24, 2014

   dx.doi.org/10.1021/nl403465v | *Nano Lett.* 2014, 14, 1714–1720

At traditional metal−semiconductor junctions (e.g., Al−Si), there is usually a SB with the Fermi level pinned in the band gap of the semiconductor at the interface region. The pinning positions vary within about 0.2 eV, independent of the metal WF, crystallographic orientation, semiconductor doping concentration, interface impurities, and so forth.[10] The formation of interfacial gap states plays a key role of FLP. As for the origins of these gap states, different mechanisms have been developed. Bardeen's theory emphasized the role of surface states in pinning the FL in band gap of semiconductors, Heine's metal-induced gap states (MIGS)[10] mechanism basically ascribed the nature of these interfacial gap states to be a decaying metallic wave function into the nanometer depth of semiconductors,[11] and high density of interface states were also found at metal− or insulator−semiconductor junctions due to defect/disorder induced gap states (DIGS).[12] It is evident that the reported partial FLP in this work is not related to any surface states and intrinsic defect or disorder (e.g., surface dangling bonds, point defects, domain boundary, and so forth) because of the modeled pristine MoS_2. Therefore, both Bardeen's theory and DIGS are not applicable in the current model study. Although being aware of the fact that the exfoliated MoS_2 is not absolutely free of defects (possibly causing contradictory findings among different experimental studies),[13] our main finding holds that even in the ideal sample without defects (or low density of defects) associated with TMDs, there is still an intrinsic partial FLP mechanism caused by metal−MoS_2 interaction. The experimentally observed metal−MoS_2 contact behaviors would be explained as a combination of the intrinsic FLP shown in this work and the extrinsic DIGS pinning mechanism. We will discuss in details in this article how the partial FLP occurs and its difference from the MIGS mechanism.

In this Letter, through a systematic first-principles study of the commensurate interfaces between single-layer MoS_2 and six types of metals (Al, Ag, Ir, Au, Pd, and Pt) with a WF spanning about 2 eV (4.2−6.1 eV), we confirm the formation of Schottky contacts in all cases. However, we find a partial FLP as the FLs of all of the examined metal−MoS_2 complexes vary in a range of 0.5−0.64 eV in the band gap with traced metal WF dependence of FLP positions. The FLP is shown to be a synergic result of two interface behaviors: metal WF modification and the interface gap states formation.

The density functional theory (DFT)[14] calculations are performed by VASP with the projector-augmented wave (PAW)[15] method. The local density approximation (LDA)[16] is used to describe the exchange-correlation functional with the partial core correction included. The (111) surfaces of metals are strained to match the optimized lattice constant of MoS_2. During the ionic relaxation of the interface structures, the shape and size of the super cell is fixed with all the atoms fully relaxed. The stopping criterion for the ionic relaxation is the remnant force on each atom below 0.01 eV/Å. A vacuum region (~27 Å) normal to the surface is added to minimize the interaction between adjacent slabs. The Monkhorst-Pack *k*-point sampling in Brillouin zone (BZ) is Γ-centered with 4 × 4 × 1 and 20 × 20 × 1 meshes in ionic and electronic optimization, respectively. The energy cutoff is chosen at 400 eV, and the electronic optimization stops when the total energies of neighboring optimization loops differ below 10^{-4} eV.

The local density approximation is appropriate for studying the metal−MoS_2 contact. GW calculations[17−20] showed that the quasiparticle energy gap for monolayer MoS_2 is ~2.6−2.8 eV, and the underestimation of the band gap by LDA or GGA is ascribed to overlooking the many body effect among electrons. An exciton binding energy of about 1.0 eV in monolayer MoS_2 results in an excitonic gap 1.8−1.9 eV observed in photoluminescence (PL) spectra. Surprisingly, PL measurements of MoS_2 samples with and without a high-K dielectric coating show the almost equal excitonic gaps with a negligible difference 30 meV.[21] The experimental evidence tends to convey a concept that the magnitude of the exciton binding energy is similar to that of the many body electron interactions within the MoS_2 sheet, resulting in PL spectra without substantial dielectric environment dependence. The strong Coulombic screening by metal slabs with infinite dielectric constant minimizes the many body effect in MoS_2,[22] rationalizing LDA and GGA calculations for metal−MoS_2 systems.[8,9] In this work, the calculated band gap of the pristine monolayer MoS_2 by LDA is 1.88 eV.

The optimized planar lattice constant of single-layer MoS_2 by LDA is 3.12 Å, close to the experimental value 3.16 Å. The maximum and minimum strain in the six metals is 6.6% compression for Al and 0.7% compression for Ir, respectively.[23] Although a small amount of strain (e.g., 0.8% by Au deposition)[22] was shown to be applied by metal deposition on monolayer MoS_2 flake, in order to catch the detailed electronic behaviors at the studied interface in a comparative manner, the lattice constant of MoS_2 is kept constant in all the metal−MoS_2 models. The side and top views of the interfaces are illustrated in Figure 1. The WF span among the six metals is about 2 eV between Al (4.2 eV) and Pt (6.1 eV), providing a good platform for exploring the energy realignment at metal−MoS_2 interfaces.

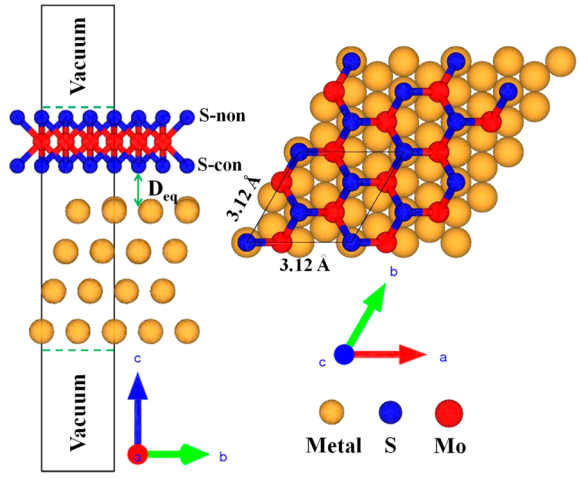

Figure 1. Side and top views of metal−MoS_2 interface. The total thickness of vacuum region is 27 Å. The black boundary indicates the super cell in simulation. "S-con" and "S-non" indicate sulfur atoms in direct contact and not in direct contact with metal slabs, respectively. Golden, blue, and orange balls represent metal contact, S, and Mo atoms, respectively.

Similar to graphene,[24,25] as shown in Table 1, MoS_2 is found to be either physisorbed or chemisorbed on the metal surfaces examined here. The s-electron metals such as Ag, Al, and Au have fully occupied d-orbitals and interact with MoS_2 weakly, whereas the d-electron metals such as Pd, Ir, and Pt interact with MoS_2 strongly. The distinct interaction strengths are well

dx.doi.org/10.1021/nl403465v | *Nano Lett.* 2014, 14, 1714−1720

Table 1. Calculated Equilibrium Interface Distance (D_{eq}), Binding Energy (BE), Work Function (WF) of Isolated Metals, Strain Applied in Metals (%), Conduction Band Offset (CBO), and Valence Band Offset (VBO) at Metal–MoS_2 Interfaces[a]

	WF (eV)	strain (%)	D_{eq} (Å)	BE (eV/S atom)	CBO[b] (eV)	VBO[b] (eV)
Al	4.24	5.6	2.88	−0.24	0.51	1.41
Ag	5.14	6.6	2.68	−0.27	0.54	1.37
Au	5.76	6.3	2.92	−0.20	0.88	0.99
Pd	5.83	1.8	2.17	−0.69	0.85	1.00
Ir	5.89	0.7	2.37	−0.56	0.86	1.15
Pt	6.12	2.5	2.48	−0.48	1.01	0.77

[a]The strain applied in all metals to match the lattice constant of MoS_2 is compressive strain. The calculated band gap edges for monolayer MoS_2 is −4.28 and −6.16 eV with the reference vacuum level at 0 eV. The Fermi levels in the six interfaces are partially pinned at 0.51–1.01 eV (0.5 eV window) below the semiconductor conduction band edge, and at 0.77–1.41 eV (0.64 eV window) above the semiconductor valence band edge. [b]Conduction and valence band edges at heterogeneous interfaces are identified by the projected main Mo d-orbital states while neglecting the minor Mo d-orbital states as gap states.

characterized by the different binding energies and equilibrium interface distances in Table 1.

The key concern for metal–semiconductor junction is the nature of the contact (viz. Ohmic versus Schottky, and n-type versus p-type). The band structures of the six metal–MoS_2 interfaces are shown in Figure 2, from which the edges of MoS_2 band gap are deduced, demonstrating the formation of Schottky contacts in all cases. As shown in the projected band structures in Figure 2, the band gap of MoS_2 is determined by the main Mo d-orbitals states (the evident black dots) at Γ-points. Because of the splitting of the states caused by the interface electronic hybridization, the extraction of the band gap size in this way has a minor degree of variance (see Figure S1 and the related text in Supporting Information). Strictly speaking, the terminology *band* is appropriate for homogeneous crystals, whereas for heterogeneous interfaces with strong orbital hybridization, the band gap of the semiconductor side can be identified by regarding the spilled hybridization states as gap states. This explains why the band gap sizes (the sum of CBO and VBO) in Table 1 vary from 1.78 to 2.01 eV. Band offset information is summarized in Table 1. Apart from platinum with the high WF of about 6.1 eV, all of the other five metals form n-type contacts. The results indicate a partial FLP behavior at the interfaces: that is, FLs are not strictly pinned at a specific energy but distribute in a 0.5–0.64 eV window in the gap for the six different contacts.

Considering that most of the studied metals have higher WFs than MoS_2, the formation of n-type contacts implies significant energy level realignment in metal–MoS_2 complexes. The decrease of the metal WF has been demonstrated at the metal-graphene interfaces due to the presence of interface dipole as a result of charge redistribution.[24−27] It has been established that, even without a notable net charge transfer between a metal substrate and an adsorbate, the surface charge repulsion effect tends to drive the charge redistribution within the two contacted materials.[27] In fact, the dipole moment of a system may have different contributions, such as from charge transfer in ionic bonded system, rearrangement of charge in covalent bonds and polarization of electronic states, etc.[28,29] Through a

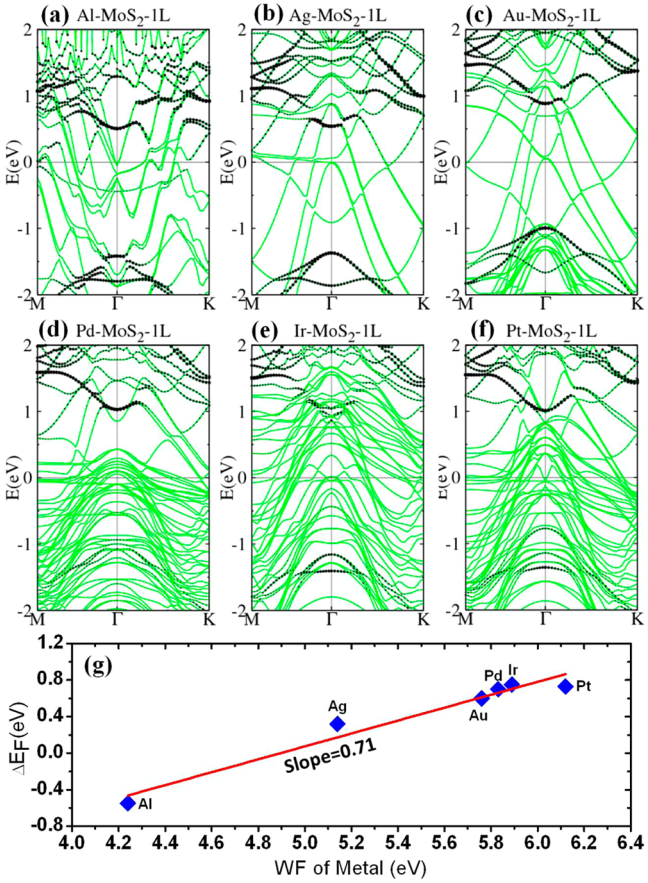

Figure 2. Band structures of single-layer MoS_2 interfacing with (a) Al, (b) Ag, (c) Au, (d) Pd, (e) Ir, and (f) Pt, respectively. (g) Summary of the relative FL shift of the contact metal upon forming a contact with MoS_2, with respect to the conduction band edges of MoS_2. The green curves in (a–f) are the overall band structures. The black dots represent the projection of Mo d-orbitals. The weight is represented by the dot size. The FL is set at E = 0 eV. The blue diamonds in (g) are simulation results and the red line is a linear fit.

similar charge difference analysis in Figure 3, a decrease of the metal WF (except Al) due to the adsorption of single-layer MoS_2 is corroborated.

Charge difference analysis is performed between complexes and isolated materials, that is, $\Delta\rho = \rho_{complex} - \rho_{Metal} - \rho_{MoS_2}$.[24] The charge density is averaged in the plane parallel to the interface. Hence, the charge redistribution along the Z-direction normal to the interface is derived. Figure 3 shows similar results to those presented by Chen et al.[8] Zooming into the details at interface region of Figure 3, the major difference for the weak metal–MoS_2 and metal–graphene contacts[25] is the presence of a charge accumulation region (red zone in Figure 3) at metal–MoS_2 interfaces. This observation is consistent with the fact that MoS_2 is chemically more reactive than graphene. The common feature for both metal–MoS_2 and metal–graphene contacts is the charge depletion region (yellow zone in Figure 3). In a general sense, both the charge depletion and the charge accumulation constitute the interface charge redistribution behavior, leading to electron wave function polarization, that is, the interface electric dipole formation. The presence of the interface dipole modifies the interface band alignment.[30]

The presence of an interface charge depletion region is direct evidence of the surface charge repulsion effect. Two dimen-

dx.doi.org/10.1021/nl403465v | *Nano Lett.* 2014, 14, 1714–1720

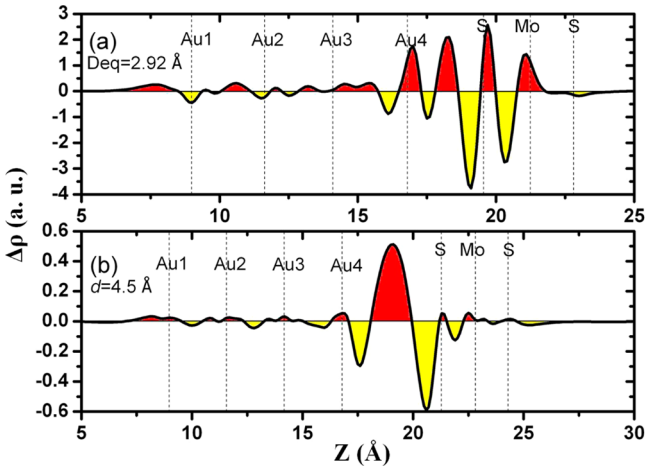

Figure 3. Plane averaged charge difference ($\Delta\rho = \rho_{complex} - \rho_{Metal} - \rho_{MoS_2}$) along the vertical *Z*-direction normal to the interface. Red color filled areas represent a charge accumulation region, and yellow color filled areas represent a charge depletion region.

sional semiconductors do not have the bulk materials' reservoir of a large amount of electrons, particularly compared to the electron sea in metals. Therefore, surface charge repulsion causes metal d-orbital rehybridization easily, leading to a larger WF change of metal (see Figure S2 and the related text in Supporting Information). Upon the modification of WFs, the FLs of the metals are raised. Therefore, aluminum with much deeper d-band than s- and p-bands would not experience the similar large WF decrease by contacting MoS_2. The quantitative calculation of the change of the dipole moments at these interfaces shows that Al experiences work function increase while other metals incur work function reduction upon MoS_2 adsorption due to the opposite interface dipole orientations (see Figure S3 and the related text in Supporting Information). The exception for the Al case is confirmed by the results in Figure 2g where the FL of Al is lowered relatively, while all the other metal FLs are raised relatively.

Quantitative analysis shows that the shift of a metal FL relative to the conduction band minimum (CBM) of MoS_2 has a linear dependence with the metal WF with a slope 0.71. If the linear dependence has a slope close to 1, the FLs of different metals would shift to the same level when in contact with MoS_2, which is an indicator of a strong FLP. Therefore, the calculated linear dependence with a slope well below unity implies that the FL is not strongly pinned at a specific energy level in band gap (see data in Table 1).

The charge accumulation region discloses another significant interface behavior: a strong metal−MoS_2 hybridization, which is further substantiated by the partial DOS (PDOS) analysis shown in Figure 4. Apparently, the direct orbital hybridization should occur between contact metals and sulfur atoms. The vertical physical separation between Mo layer and the metal slab is 3.73−4.48 Å for the six studied metals, larger than the van der Waals separation (for example, in graphite) 3.34 Å. Therefore, there is no direct wave function overlap, and correspondingly a direct hybridization of Mo and metal electronic states is not anticipated. However, a detailed PDOS analysis reveals that the gap states are predominantly of Mo d-orbitals character with larger contribution in the upper part of the MoS_2 band gap. In the PDOS profiles of Figure 4, the similarity between Mo d-orbitals and contact metals d-orbitals indicates the strong correlation between contact metals

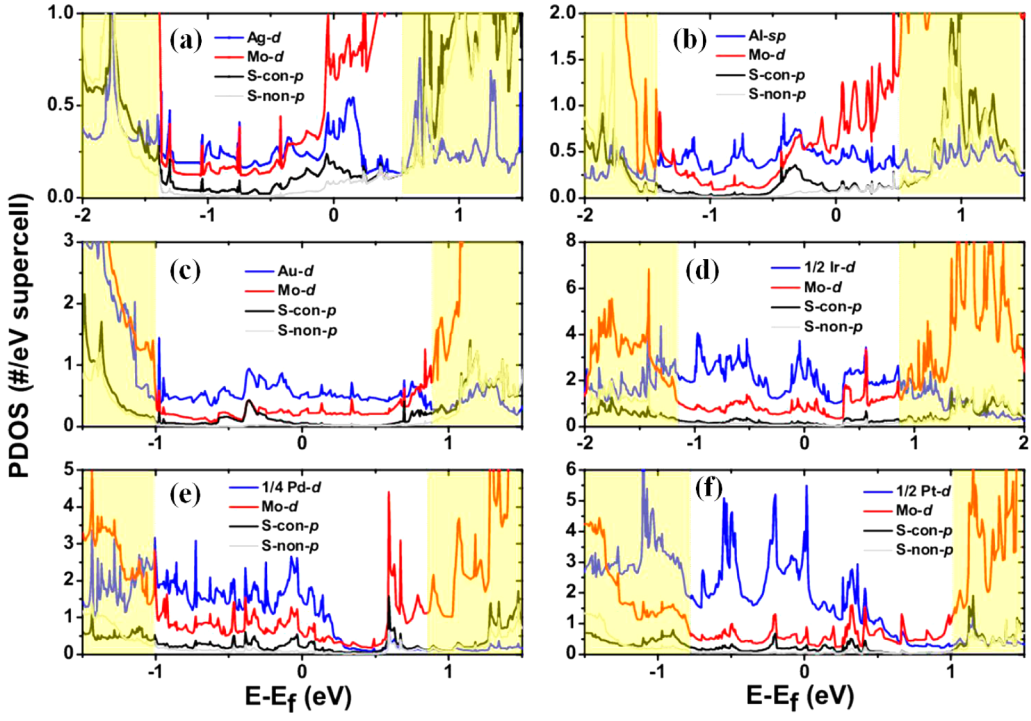

Figure 4. PDOS of metal−MoS_2 interfaces for (a) Ag, (b) Al, (c) Au, (d) Ir, (e) Pd, and (f) Pt, respectively. The yellow shaded zone in each figure indicates the conduction band and valence band edges, determined by the Mo d-orbitals projection in the band structures, as shown in Figure 2. "1/2 Ir-d" in (d) means the d-orbital DOS of surface Ir atoms is intentionally reduced to half in plot for comparison with other curves. 1/4 Pd in (e) and 1/2 Pt in (f) are similarly represented.

dx.doi.org/10.1021/nl403465v | *Nano Lett.* 2014, 14, 1714−1720

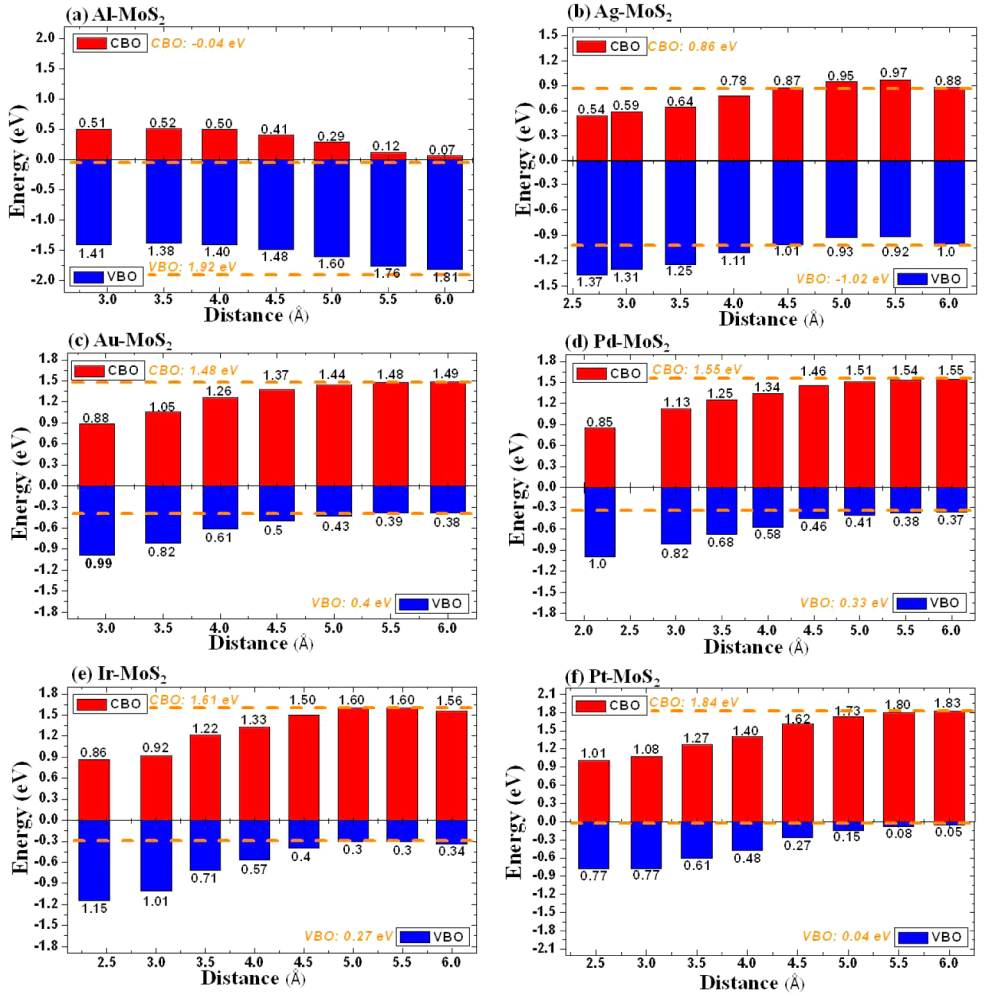

Figure 5. Interface separation dependence of CBO and VBO for (a) Al, (b) Ag, (c) Au, (d) Pd, (e) Ir, and (f) Pt electrodes interfacing with monolayer MoS_2. FL is at $E = 0$ eV. The first color bar in the left of each figure corresponds to the equilibrium interface distance. Orange horizontal dashed lines in each figure indicate the CBO and VBO simply derived from isolated metal slabs and MoS_2, based on the conventional Schottky–Mott model. In (a), the negative CBO represented by the dashed line means the FL of Al is higher than the CBM of MoS_2.

and Mo atoms. Essentially, Figure 4 shows more Mo d-states than S sp-states in the band gap.

Sulfur atoms play a role of mediating the hybridization between metal and Mo atoms, resulting in the production of gap states. It is well-known that the gap size of single-layer MoS_2 is critically determined by the Mo–S covalent bonding strength, and band gap edges of single-layer MoS_2 is over 80% constituted of Mo d-orbitals.[20] For convenience, we denote the sulfur atoms in direct contact with metal layers as S_{con}, while the sulfur atoms at the vacuum side is termed as S_{non}, as shown in Figure 1. The metal contacts disturb the electron distribution surrounding S_{con} atoms, thus affecting the S_{con}–Mo bonding. The interfacial metal-S bonding weakens the intralayer S_{con}–Mo bonding, and thus the Mo d-states at the band edges spread into the band gap, producing gap states, which is essential for pinning the FL. Therefore, albeit the interatomic contact occurs between metals and S_{con} instead of Mo, gap states are predominantly formed by the Mo d-orbitals. This mechanism is similar to the band gap reduction of MoS_2 by interlayer interaction with increasing number of layers in which conduction band edge is lowered to reduce the band gap from 1.8 eV (for 1 ML) to 1.2 eV (for bulk). The dominant contribution of Mo d-orbitals in the upper part of the band gap explains the driving force to pin the Fermi level in the upper half of the band gap forming n-type Schottky contacts (Figure 5). Note that the overall effect of the presence of the interface metal-S bonding weakens the intralayer S–Mo bonding, spilling band edge states into the gap regions. However, the identification of band edges is by adopting the main Mo d-orbitals states at the specific Γ-point while neglecting the minor Mo d-orbitals states as gap states (see Figure S1 and the related text in Supporting Information). Hence, it is possible that some derived band gap sizes appear to be enlarged as indicated in Table 1.

Electronic features at metal–MoS_2 interfaces uncover the difference of the partial FLP mechanism from the MIGS. Albeit minor, there is still a noticeable metal WF dependence of the pinned FLs with 0.5–0.64 eV variance, which spans almost one-third of the band gap. Another striking feature is the favored localization of gap states at Mo atoms instead of S_{con} atoms, deviating from the behavior of the decaying wave function of metals.[11] MIGS is therefore not applicable for the reported partial FLP.

Increased separation of metal contact from MoS_2 weakens the modification of the metal WFs and meanwhile mitigates the interface hybridization resulting in fewer gap states and thus

dx.doi.org/10.1021/nl403465v | Nano Lett. 2014, 14, 1714–1720

unpinning the FL. As shown in Figure 3b, when the interface separation is increased to 4.5 Å, the degree of charge redistribution is largely decreased, evidenced by an order of magnitude smaller *y*-axis values. Figure 5 shows that with 6.0 Å interface separation, all contacts obey the quantitative prediction of the conventional Schottky−Mott model which dictates the SBH solely by the WF difference of isolated materials. It suggests an insertion of appropriate buffering materials between metals and MoS_2 would be a promising technique for unpinning the FLs.[31]

In summary, a systematic DFT study of monolayer MoS_2 was conducted interfacing it with six contact metals spanning about 2 eV WF difference. The large deviation of the band alignment at the metal−MoS_2 interfaces from the prediction of conventional Schottky-Mott model suggests significant band realignment caused by interface dipole formation. Similar to graphene, the adsorption of MoS_2 modifies the WF of the metals through an interface dipole formation resulting from notable interface charge redistribution. Moreover, the formation of gap states, mainly of Mo d-orbitals character, is found as a result of sulfur-mediated interface hybridization. Metal adsorption weakens the S−Mo intralayer bonding, spreading the band edge states (mainly Mo d-orbitals) into the band gap. The modified WF at the metal side and the presence of gap states at MoS_2 side synergistically result in a partial Fermi level pinning at metal−MoS_2 interfaces, which is intrinsically different from Bardeen's theory, MIGS, and DIGS. Through the understanding of the origin of this partial Fermi level pinning, we can develop new ideas to form Ohmic junctions between metal and TMD semiconductors.

■ ASSOCIATED CONTENT

Supporting Information

Projected Mo d-orbitals states at Au−MoS_2 interfaces; density of states of each sub-d-orbitals of surface Au atoms; calculation of the dipole moments at the studied interface. This material is available free of charge via the Internet at http://pubs.acs.org.

■ AUTHOR INFORMATION

Corresponding Author

*E-mail: kjcho@utdallas.edu.

Notes

The authors declare no competing financial interest.

■ ACKNOWLEDGMENTS

The authors acknowledge useful discussions with Professor C. Hinkle and Dr. S. McDonnell. This work was supported by the Center for Low Energy Systems Technology (LEAST), one of six centers supported by the STARnet phase of the Focus Center Research Program (FCRP), a Semiconductor Research Corporation program sponsored by MARCO and DARPA. K.C. is partially supported by Nano·Material Technology Development Program through the National Research Foundation of Korea (NRF) funded by the Ministry of Science, ICT and Future Planning (2012M3A7B4049888).

■ REFERENCES

(1) Radisavljevic, B.; Radenovic, A.; Brivio, J.; Giacometti, V.; Kis, A. Single-layer MoS_2 transistors. *Nat. Nanotechnol.* **2011**, *6*, 147−150.

(2) Jena, D.; Konar, A. Enhancement of carrier mobility in semiconductor nanostructures by dielectric engineering. *Phys. Rev. Lett.* **2007**, *98*, 136805.

(3) Liu, H.; Neal, A. T.; Ye, P. D. Channel length scaling of MoS_2 MOSFETs. *ACS Nano* **2012**, *6*, 8563−8569.

(4) Neal, A. T.; Liu, H.; Gu, J. J.; Ye, P. D. In Metal contacts to MoS_2: A two-dimensional semiconductor; *Device Research Conference*; University Park, TX, June 18-20, 2012; pp 65−66.

(5) Das, S.; Chen, H. Y.; Penumatcha, A. V.; Appenzeller, J. High-performance multilayer MoS_2 transistors with scandium contacts. *Nano Lett.* **2013**, *13*, 100−105.

(6) Fontana, M.; Deppe, T.; Boyd, A. K.; Rinzan, M.; Liu, A. Y.; Paranjape, M.; Barbara, P. Electron-hole transport and photovoltaic effect in gated MoS_2 Schottky junctions. *Sci. Rep.* **2013**, *3*, 1634.

(7) Qiu, H.; Pan, L. J.; Yao, Z. N.; Li, J. J.; Shi, Y.; Wang, X. R. Electrical characterization of back-gated bi-layer MoS_2 field-effect transistors and the effect of ambient on their performances. *Appl. Phys. Lett.* **2012**, *100*, 123104.

(8) Chen, W.; Santos, E. J. G.; Zhu, W. G.; Kaxiras, E.; Zhang, Z. Y. Tuning the electronic and chemical properties of monolayer MoS_2 adsorbed on transition metal substrates. *Nano Lett.* **2013**, *13*, 509−514.

(9) Popov, I.; Seifert, G.; Tomanek, D. Designing electrical contacts to MoS_2 monolayers: A computational study. *Phys. Rev. Lett.* **2012**, *108*, 156802.

(10) Heine, V. Theory of surface states. *Phys. Rev.* **1965**, *138*, A1689.

(11) Louie, S. G.; Cohen, M. L. Self-consistent pseudopotential calculation for a metal-semiconductor interface. *Phys. Rev. Lett.* **1975**, *35*, 866−869.

(12) Hasegawa, H.; Sawada, T. On the electrical-properties of compound semiconductor interfaces in metal-insulator semiconductor structures and the possible origin of interface states. *Thin Solid Films* **1983**, *103*, 119−140.

(13) Zhou, W.; Zou, X. L.; Najmaei, S.; Liu, Z.; Shi, Y. M.; Kong, J.; Lou, J.; Ajayan, P. M.; Yakobson, B. I.; Idrobo, J. C. Intrinsic structural defects in monolayer molybdenum disulfide. *Nano Lett.* **2013**, *13*, 2615−2622.

(14) Kresse, G.; Furthmuller, J. Efficiency of ab-initio total energy calculations for metals and semiconductors using a plane-wave basis set. *Comput. Mater. Sci.* **1996**, *6*, 15−50.

(15) Blochl, P. E. Projector augmented-wave method. *Phys Rev. B* **1994**, *50*, 17953−17979.

(16) Ceperley, D. M.; Alder, B. J. Ground-state of the electron-gas by a stochastic method. *Phys. Rev. Lett.* **1980**, *45*, 566−569.

(17) Cheiwchanchamnangij, T.; Lambrecht, W. R. L. Quasiparticle band structure calculation of monolayer, bilayer, and bulk MoS_2. *Phys. Rev. B* **2012**, *85*, 205302.

(18) Shi, H. L.; Pan, H.; Zhang, Y. W.; Yakobson, B. I. Quasiparticle band structures and optical properties of strained monolayer MoS_2 and WS_2. *Phys. Rev. B* **2013**, *87*, 155304.

(19) Liang, Y.; Huang, S.; Soklaski, R.; Yang, L. Quasiparticle band-edge energy and band offsets of monolayer of molybdenum and tungsten chalcogenides. *Appl. Phys. Lett.* **2013**, *103*, 042106.

(20) Gong, C.; Zhang, H.; Wang, W.; Colombo, L.; Wallace, R. M.; Cho, K. Band alignment of two-dimensional transition metal dichalcogenides: Application in tunnel field effect transistors. *Appl. Phys. Lett.* **2013**, *103*, 053513.

(21) Yan, R.; Bertolazzi, S.; Brivio, J.; Fang, T.; Konar, A.; Birdwell, A. G.; Nguyen, N. V.; Kis, A.; Jena, D.; Xing, H. Raman and photoluminescence study of dielectric and thermal effects on atomically thin MoS_2. arXiv:1211.4136, 2013.

(22) Gong, C.; Huang, C.; Miller, J.; Cheng, L.; Hao, Y.; Cobden, D.; Kim, J.; Ruoff, R. S.; Wallace, R. M.; Cho, K.; Xu, X.; Chabal, Y. J. Metal contacts on physical vapor deposited monolayer MoS_2. *ACS Nano* **2013**, *7*, 11350−11357.

(23) The electronic structures of metal with strain are very close to the unstrained system. Therefore, the metal strain effect does not change the finding of the current interface model study.

(24) Giovannetti, G.; Khomyakov, P. A.; Brocks, G.; Karpan, V. M.; van den Brink, J.; Kelly, P. J. Doping graphene with metal contacts. *Phys. Rev. Lett.* **2008**, *101*, 026803.

(25) Gong, C.; Lee, G.; Shan, B.; Vogel, E. M.; Wallace, R. M.; Cho, K. First-principles study of metal-graphene interfaces. *J. Appl. Phys.* **2010**, *108*, 123711.
(26) Gong, C.; Hinojos, D.; Wang, W. C.; Nijem, N.; Shan, B.; Wallace, R. M.; Cho, K. J.; Chabal, Y. J. Metal−Graphene-Metal sandwich contacts for enhanced interface bonding and work function control. *ACS Nano* **2012**, *6*, 5381−5387.
(27) Bagus, P. S.; Staemmler, V.; Woll, C. Exchangelike effects for closed-shell adsorbates: Interface dipole and work function. *Phys. Rev. Lett.* **2002**, *89*, 096104.
(28) Leung, T. C.; Kao, C. L.; Su, W. S.; Feng, Y. J.; Chan, C. T. Relationship between surface dipole, work function, and charge transfer: some exceptions to an established rule. *Phys. Rev. B* **2003**, *68*, 195408.
(29) Chan, K. T.; Neaton, J. B.; Cohen, M. L. First-principles study of metal adatom adsorption on graphene. *Phys. Rev. B* **2008**, *77*, 235430.
(30) Tung, R. T. Formation of an electric dipole at metal-semiconductor interfaces. *Phys. Rev. B* **2001**, *64*, 205310.
(31) Yang, H.; Heo, J.; Park, S.; Song, H. J.; Seo, D. H.; Byun, K. E.; Kim, P.; Yoo, I.; Chung, H. J.; Kim, K. Graphene barristor, a triode device with a gate-controlled Schottky barrier. *Science* **2012**, *336*, 1140−1143.